

Learning Global Inverse Statics Solution for a Redundant Soft Robot

Thomas George Thuruthel¹, Egidio Falotico¹, Matteo Cianchetti¹, Federico Renda²
and Cecilia Laschi¹

¹*The Biorobotics Institute, Scuola Superiore Sant'Anna, Pisa, Italy*

²*KURI Institute, Khalifa University, Abu Dhabi, U.A.E.*

Keywords: Soft Robots, Machine Learning, Inverse Statics, Inverse Dynamics, Steady State Model, Neural Networks.

Abstract: This paper presents a learning model for obtaining global inverse statics solutions for redundant soft robots. Our motivation begins with the opinion that the inverse statics problem is analogous to the inverse kinematics problem in the case of soft continuum manipulators. A unique inverse statics formulation and data sampling method enables the learning system to circumvent the main roadblocks of the inverting problem. Distinct from previous researches, we have addressed static control of both position and orientation of soft robots. Preliminary tests were conducted on the simulated model of a soft manipulator. The results indicate that learning based approaches could be an effective method for modelling and control of complex soft robots, especially for high dimensional redundant robots.

1 INTRODUCTION

Continuum soft robots are a class of robots made of soft materials that exhibit highly dexterous and adaptive behaviour. Not a lot is known about the dynamic behaviour of continuum robots. They are inherently difficult to control, due to their compliance. However, they have some characteristics which make certain tasks easier for them. Their compliant nature makes them frontrunners for applications involving interactions with delicate or unstructured environment (Rus et al., 2015).

As a growing field in robotics, there are numerous challenges restricting the application of soft robots. One of them is the construction of inverse models for their kinematic and dynamic behaviour. IK models have the advantage that their solutions are load independent. However, our interest lies on modelling the inverse steady state dynamics (statics) of these robots, specifically for redundant soft manipulators. We believe that hybrid controllers with coupled inverse kinematic solvers and inverse statics (IS) solvers would be exciting for soft robotics applications. They can be used in tandem for position control and force/stiffness estimation.

Theoretically, due to their continuous nature, soft robots have an infinite number of degrees of

freedom, making them under-actuated. Assuming that there are no external forces, we can still develop a mapping between the applied internal forces and the configuration of the robot very much like the case of kinematics. However, developing an inverse model poses more difficulties. Similar to the inverse kinematic formulation of rigid redundant robots, the inverse statics solution is not unique and the solution set forms a non-convex set (D'Souza et al., 2001). Furthermore, analytical or numerical methods appear to be very complex unless developed with simplified models (Marchese et al., 2014). We are, therefore, adopting a method based on machine learning for estimating these models.

Inverse statics models are meaningful only for soft manipulators and parallel robots because of the existence of a stable zero velocity fixed point. Essentially, the IS model is analogous to the IK model for rigid robots. Therefore, numerous approaches developed for IK problem of redundant rigid robots can be directly used for our case. Among the learning based approaches, a common theme is the use of locally linear models and stitching them together to form a global estimate. This can be done in the velocity level and has been widely used (D'Souza et al., 2001; Susumu et al., 2001; DeMers et al., 1992). However, differential IK methods involve integration over time to obtain position estimates which can lead to accumulation of

errors. Alternatively, a position level IK solution was proposed using goal babbling (Rolf et al., 2013a). However, this method generates only a particular global solution and requires lot of sample data. Inverting a learned forward model was carried out by distal supervised learning by few researchers (Jordan et al., 1992; Melingui et al., 2014). However, these methods have not scaled well for higher dimensional systems. Position level IK solution has been proposed using modular learning architectures by few other researchers (Vannucci et al., 2014; 2015), but it involves very complex constructions.

In this paper we propose an approach for learning the global inverse statics model for a continuum robot. Our method is also based on the locally linear and convex properties of the IS solution. However, we further utilize the fact that these local models can be scaled and used as a decent approximation of the global solution. This can be achieved by appropriate biasing and selection of the input/output representation of the learning system. We are using neural networks to approximate the proposed IS mapping. Giorelli et al., (2015), were one of the first researchers to propose the learning of the inverse statics of soft arm. They were successfully able to learn the inverse statics for the position control of a soft robot. However, their study was limited to the case of a non-redundant manipulator and further restricted to only position control (three Degrees of Freedom). Therefore, this paper proposes a method for obtaining the global solutions for both position and orientation of a soft redundant robot. We have tested and validated the proposed method on a simulated steady state model of a 12 Degrees of Freedom (DoF) soft manipulator. We have tried to show by simulations that the proposed method performs soundly even with the issues of redundancy and high dimensionality. Further, we try to investigate the underlying form of the learned system and compare it with the commonly used inverse Jacobian based method.

2 PROPOSED METHOD

The forward static model or steady state model can be represented by:

$$\mathbf{x} = f(\mathbf{q}) \quad (1)$$

Where, $\mathbf{x} \in \mathcal{R}^m$ is the position and orientation vector; $\mathbf{q} \in \mathcal{R}^n$ is the vector containing the actuator tensions; and f is some surjective function. This particular representation is not invertible when $m < n$ (redundant). As mentioned before, we can develop

local representations by linearizing the function at a point (\mathbf{q}^o), thereby obtaining;

$$\delta\mathbf{x} = J(\mathbf{q}^o)\delta\mathbf{q} \quad (2)$$

Here, $J(\mathbf{q}^o)$ is the Jacobian matrix at the point \mathbf{q}^o ; $\delta\mathbf{x}$ and $\delta\mathbf{q}$ are infinitesimally small changes in \mathbf{x} and \mathbf{q} respectively. The differential IK method involves generating samples of $(\delta\mathbf{x}, \delta\mathbf{q}, \mathbf{q})$ and learning the mapping $(\delta\mathbf{x}, \mathbf{q}^o) \rightarrow \delta\mathbf{q}$. The learning is feasible since the differential IK solutions form a convex set and therefore averaging multiple solutions still results in a valid solution (D'Souza et al., 2001). The method we have proposed involves expanding Eq. 2 and expressing it in terms of absolute positions, as shown below:

$$J(\mathbf{q}_i)\mathbf{q}_{i+1} = \mathbf{x}_{i+1} - f(\mathbf{q}_i) + J(\mathbf{q}_i)\mathbf{q}_i \quad (3)$$

Here, \mathbf{q}_{i+1} is the next actuator configuration for reaching a point \mathbf{x}_{i+1} from the present configuration \mathbf{q}_i . Note that Eq. 3 is only valid when the configurations are infinitesimally close. However, for practical purposes this can be a good approximation for larger regions. The analytical solution for Eq. 3 can be written as:

$$\mathbf{q}_{i+1} = G(\mathbf{x}_{i+1} - f(\mathbf{q}_i) + J\mathbf{q}_i) + (I_n - GJ)\mathbf{z} \quad (4)$$

Where, G , is a generalized inverse of $J(\mathbf{q}_i)$ and I_n is the identity matrix and \mathbf{z} is an arbitrary n -dimensional vector. The first component represents the particular solution to the non-homogenous problem prescribed in Eq. 3 and the second component represents the infinite homogenous solutions. It can be proved that the solution space still forms a convex set. Therefore, any universal function approximator can be used for learning the mapping $(\mathbf{q}_i, \mathbf{x}_{i+1}) \rightarrow (\mathbf{q}_{i+1})$. Setting the vector \mathbf{z} to zero and using the Moore-Penrose pseudoinverse provides us with the minimum norm ($\|\mathbf{q}_{i+1}\|$) solution to the linear eq. 3.

The samples $(\mathbf{q}_i, \mathbf{q}_{i+1}, \mathbf{x}_{i+1})$ generated are such that $\|\mathbf{q}_{i+1} - \mathbf{q}_i\| < \epsilon$. An appropriate value of ϵ is between 10% – 5% of the maximum actuator range. The advantage of this reformulation is in the simple detail that the input/ output domain of the learning system is now same as the actuator space and task space configuration and not a subset of it, unlike the differential IK method. We predict that this way our proposed method will behave exactly like the differential IK method at local regions and at farther points they will automatically provide approximate configurations that will bring the end effector configuration closer to the target. Therefore if we repeat the process for a fixed target, we can expect the process to converge near the target position.

Therefore, by our method we can get global solutions for the IS problem. We can further add constraints during the iteration process to develop particular solutions for the IS problem according to our requirement.

2.1 Reachability and Workspace Considerations

Since, the IS solution will provide the actuator configuration to take the end effector to a particular position and orientation, it is important to know if the input arguments (\mathbf{x}_{i+1}) given to the system is reachable. For the case of end effector position, the reachable workspace will describe the volume in which the end effector position can reach. The reachable workspace can be estimated easily either by analytical, numerical or experimental methods. However, the dextrous workspace, which describes the volume in which the end effector can reach with all orientations, is much more difficult to find. Nonetheless, the calculation of the dextrous workspace is not of significance for soft robots. Dextrous workspace is a property introduced primarily for rigid robots with spherical joints. For soft robots, the manifold of reachable orientation varies according to the end effector position.

Interestingly, there exists a single unique manifold for each position, unlike the case of rigid robots which can have multiple disjoint manifolds (Kapadia et al., 2013). This is attributed to the fact that for soft continuum robots, singular configurations arise only when the manipulator has zero curvature. Singularities at boundaries can be ignored since the manipulator can, theoretically, extend or contract to any length. Furthermore, in our formulations, we are neglecting rotations along the backbone of the robot (roll). So, our robot can be visualized as a ‘pointing’ robots (rotations in $SO(3)$ are replaced by directions in S^2). By this process our formulation is theoretically devoid of singularities. This implies that given a current position and orientation ($\mathbf{x}_0^p, \mathbf{x}_0^o$), there exists a continuous path in the actuator space, which can bring the end effector to a different orientation ($\mathbf{x}_1^p, \mathbf{x}_1^o$), without affecting the position. Learning the null space solution for each end effector configuration will help us in implementing this. However, learning the null space from just experimental data is very difficult. Therefore, in this paper we have developed two solvers for the IS problem; one for both position and orientation and the other for just the orientation. These two solvers can be combined appropriately to attain the required

accuracies in position and orientation. For instance, if the network output for coupled (position + orientation) IS solver is \mathbf{q}_{i+1}^c and the output for Inverse Orientation Statics (IOS) solver is \mathbf{q}_{i+1}^o , then, they can be combined to give actuator configuration \mathbf{q}_{i+1}^a , where;

$$\mathbf{q}_{i+1}^a = k * \mathbf{q}_{i+1}^c + (1 - k) * \mathbf{q}_{i+1}^o \quad (5)$$

By regulating the value of the constant k ($k \leq 1$), we can accordingly vary the orientation accuracy. In further sections we will be referring to this formulation as the appended IS solver and the complete IS solver will be just referred to as the IS solver.

3 STEADY STATE MODEL

The constant curvature model is the most widely used construction technique for soft robots due to their simplicity and computational ease (Walker, 2013). Non- constant curvature models based on cosserat beam dynamics promises to be a better alternative (Renda et al., 2014). For our application, we have used a steady state model of a tendon driven soft continuum robot (Renda et al., 2012). The sample data for learning the IS model is obtained from this steady state model.

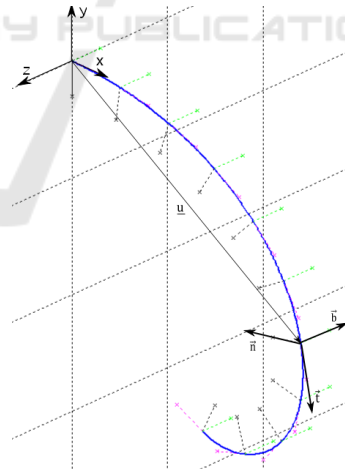


Figure 1: Kinematic representation of the cosserat beam model.

The soft continuum robot is modelled as a cosserat beam. A cosserat beam can be visualized as a continuum body which is composed of infinitesimally small rigid bodies that can rotate independently from the neighbouring element. The position and orientation of each material element is

represented by four vectors: $\mathbf{u}, \mathbf{t}, \mathbf{n}, \mathbf{b}$. The unit vector \mathbf{t} is tangential to the manipulator backbone at that section and the vectors \mathbf{n} and \mathbf{b} lie on the cross sectional area of the element. These three unit vectors form the local reference frame for each element. Therefore, the relation $\mathbf{b} = \mathbf{t} \times \mathbf{n}$ holds true everywhere. \mathbf{u} is the position vector of the centre of mass of an element (Fig. 1). We are ignoring the effects of shear stresses in our formulation (Euler-Bernoulli hypothesis). This restricts the DoF of each element to four. The total length of our manipulator is 31 centimetres, divided into a section per centimetre.

The complete configuration of the robot can be calculated by obtaining the four vectors for each element. The elements are related to each other in space by the below equations (Renda et al., 2012):

$$\frac{d\mathbf{t}}{ds} = k(s)(1 + q(s))\mathbf{n}(s) - \xi(s)(1 + q(s))\mathbf{b}(s) \quad (6)$$

$$\frac{d\mathbf{n}}{ds} = -k(s)(1 + q(s))\mathbf{t}(s) - \tau(s)(1 + q(s))\mathbf{b}(s) \quad (7)$$

$$\frac{d\mathbf{n}}{ds} = \xi(s)(1 + q(s))\mathbf{t}(s) - \tau(s)(1 + q(s))\mathbf{n}(s) \quad (8)$$

$$\frac{d\mathbf{u}}{ds} = (1 + q(s))\mathbf{t}(s) \quad (9)$$

Here the functions $k(s)$ and $\xi(s)$ are the curvatures with respect to $\mathbf{b}(s)$ and $\mathbf{n}(s)$, $\tau(s)$ is the torsion with respect to $\mathbf{t}(s)$, and $q(s)$ is the longitudinal strain along the arm. s , is the parametrization variable which represents an element.

The variables $k(s)$, $\xi(s)$, $\tau(s)$ and $q(s)$ are related by the following equations:

$$\begin{pmatrix} GI & 0 & 0 \\ 0 & EJ_n & 0 \\ 0 & 0 & EJ_b \end{pmatrix} \begin{pmatrix} \frac{d\tau}{ds} \\ \frac{d\xi}{ds} \\ \frac{dk}{ds} \end{pmatrix} + \begin{pmatrix} GI & 0 & 0 \\ 0 & EJ_n & 0 \\ 0 & 0 & EJ_b \end{pmatrix} \begin{pmatrix} \tau \\ \xi \\ k \end{pmatrix} \quad (10)$$

$$= \dot{\mathbf{M}}(s) \\ EAq(s) = N(s) \quad (11)$$

Where, $N(s)$ is the \mathbf{t} component of the internal contact forces and $\mathbf{M}(s)$ is the vector of the internal torque forces (The dot symbol is the derivative with respect to s). E is the Young's modulus, G is the shear modulus, I , J_n and J_b are the moment of inertia of the section with respect to \mathbf{t} , \mathbf{n} and \mathbf{b} , in that order. The internal contact forces and the internal torque forces are calculated based on the cable configuration and tension on each cable (Refer to Renda et al., 2012). Equation 10 is numerically integrated from tip to base and solved along with

equation 11 and appropriate boundary conditions to obtain the curvatures and strains in each segment. Finally, the kinematic equations 6, 7, 8, 9 are integrated to obtain the arm shape.

There are three anchorage planes along the length of the manipulator. Each anchorage plane has four cables attached to it; each spaced apart by an angle of 90 degrees. Fig. 2 shows the reachable workspace of the robot obtained by random exploration in the actuator space.

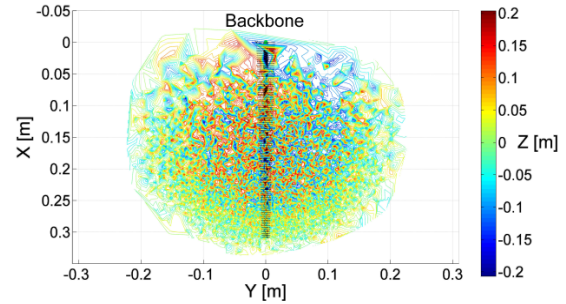


Figure 2: Schematic of the robot end effector workspace.

4 DATA COLLECTION AND TRAINING

The samples $(\mathbf{q}_i, \mathbf{q}_{i+1}, \mathbf{x}_{i+1})$ are generated by motor babbling. The distance between consecutive samples $(\mathbf{q}_{i+1} - \mathbf{q}_i)$ is decided randomly from a range to avoid any bias in the sample. The range of the each sampling data is from zero to 8 percent of the maximum actuator force. The range is decided by trial and error. Learning with a lower range will give better accuracy, but requires larger data set and performs poorly for farther target points. Therefore a continuous path must be planned beforehand, just like the case of differential IK. Selecting the distance from a range rather than a fixed value keeps the continuous nature of the problem intact, at least partially. Note that there are 12 actuators which can select its actions continuously. Even if we consider that the actuator space is discretized into 12 segments (each segment being roughly 8 percentage of the total range), there are still around $9e+12$ possible configurations. Therefore, we cannot navigate the whole actuator space, instead we expect the generalization ability of neural networks or other machine learning process's to predict accurate solutions for unseen data.

4.1 Training

As mentioned before, we are using neural networks

to learn the mapping $(\mathbf{q}_i, \mathbf{x}_{i+1}) \rightarrow (\mathbf{q}_{i+1})$. The input layer is of size 18 for the IS solver and 15 for the IOS solver. The output layer size is 12 for both cases. We are using a multilayer perceptron with a single hidden layer for this. Tan-sigmoid activation function is used in the hidden layer and a linear activation function is used at the output layer. Proper care must be taken during the training process. Bayesian regularization backpropagation method is used for training the neural network (Foresee et al., 1997). The inputs and outputs are normalized and divided randomly in the pre-processing stage. A uniformly distributed noise is also added to the inputs to imitate realistic scenarios. The magnitude of the noise goes up to 3% of the maximum sampling range. Since the Bayesian regularization backpropagation algorithm is used for training; the data set is divided into training and test set in the ratio 80:20. No validation set is used. In the following subsections we describe the methodology adopted for determining the network size and sample data size for learning the IS. The parameters of the IOS solver are adopted from the IS solver as it can be seen as a subset of the IS problem.

4.1.1 Network Size

Proper care must be given to decide the hidden layer size. It is not enough to get good training or test performance, contrary to common intuition. The learning task provided to the neural networks is to learn a left inverse function. However, our objective is to learn the right inverse function (Rolf et al., 2013b). In other words, the neural network tries to reduce the error between the predicted values of $\mathbf{q}_{i+1}(\mathbf{q}^p)$ and the sample values of $\mathbf{q}_{i+1}(\mathbf{q}^s)$. Whereas, the final aim is to reduce the error between $f(\mathbf{q}^p)$ and \mathbf{x}_{i+1} . There are local minima which can provide good training and test performance, and still perform poorly as a IS solver. For instance, a network that outputs $\mathbf{q}_{i+1} = \mathbf{q}_i$, can give good training and test performance as both values are nearby due to the sampling method. Therefore, the appropriate size for the network is decided by checking the training error along with the performance of the IS solver. Fig.3 shows effect of network size on the training performance and the corresponding change in the IS performance. IS solver performance is measured by testing the solutions for fifty points randomly selected from the sample data (to ensure that the targets are reachable).

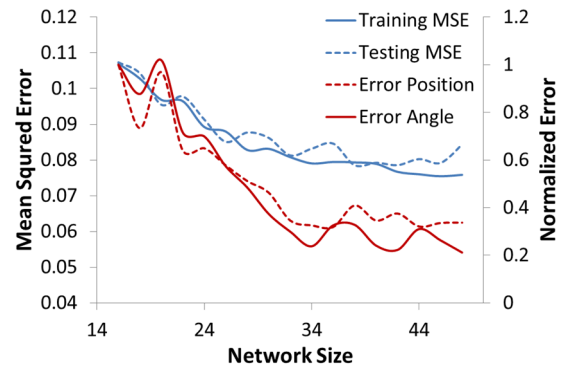


Figure 3: Network size determination. The errors in position and angle are normalized for easier comparison.

4.1.2 Sample Size

The length of the sample data required would be directly proportional to the number of DoF's of the system. Fig. 4 shows how the number of samples determine the performances of the network and the IS solver.

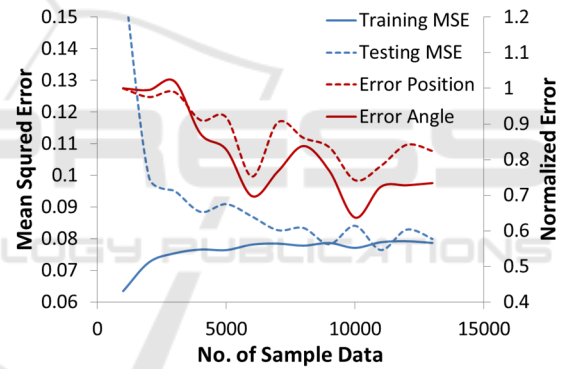


Figure 4: Sample data size determination. The network size is forty for all tests.

For all the ensuing experiments we have selected 14000 samples for training a neural network of size 40 units. Note that the proposed method needs to explore only a miniscule percentage of the actuator space. The same analysis cannot be done independently for IOS solver since the performance of the IOS solver is heavily dependent on the position of the manipulator (Reachability of a particular orientation depends on the corresponding position). Therefore, the performance of the IOS solver can only be inspected with the help of the IS solver. However, since we are using Bayesian regularization backpropagation algorithm for training the network, an exaggerated network size and sample data will not harm the learning process. Therefore, the same parameters of the IS solver was adopted for the IOS solver.

5 RESULTS AND ANALYSIS

This section is divided into three subsections; the first subsection shows the test results for the developed IS solver on the simulated steady state model; the second subsection discusses the results with the appended IS solver (Sec. 2.1); the final subsection makes a comparative analysis of the proposed method with the inverse Jacobian method. There are two reasons for this; the first one is to compare the performance of the two methods; secondly, the comparison can help us understand the underlying form of the learned network.

5.1 Simulations

The main advantage of the proposed method is its ability to provide global solutions to the IS problem without the need to pre-plan a path from the starting point. So, the first tests were to evaluate if the IS solver can provide accurate actuator configuration for random target points in the workspace. Fifty points ($x \in (-0.05, 0.35), y \in (-0.25, 0.25), z \in (-0.2, 0.2)$) were randomly selected from the sample data along with their corresponding orientation. Since the target points are not close to the home position (0.31[m], 0[m], 0[m]), the solver needs more than one iteration for converging to the right solution. Fig. 5 shows the test results for this experiment. The proposed method is able to generate results with a mean positional error of 0.012 meters and mean orientation error of 7.4 degrees. The method converges with an average of 3.56 steps for convergence within a range of 1mm. The same fifty target points were again used in the IS solver for a starting point at one of the extreme boundary points (-0.02[m], -0.16[m], -0.01[m]). The corresponding results are shown in Fig. 6. The average errors increase in this case. The average positional error goes to 0.015 meters and the average orientation error goes to 9.92 degrees. The convergence speed remains the same with each target taking an average of 3.68 iterations for convergence. Note that even though the magnitude of error increases, the error pattern remains relatively similar. We suggest that these points are under-represented in the sample data and therefore the learning system does not have an adequate representation around that region. One possible work-around is to develop algorithms that perform motor babbling initially and then later switch to a more goal oriented exploration strategy.

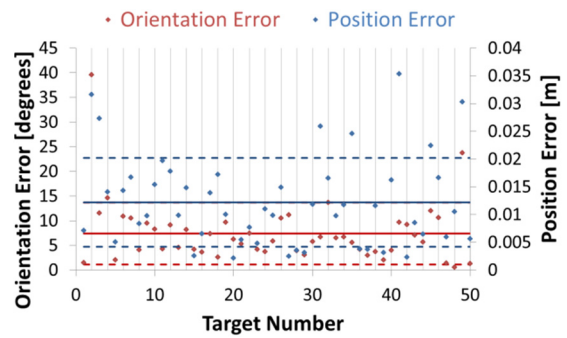


Figure 5: Simulation results for the fifty points experiment at the natural starting point. The thick lines represent the mean of the data and the dotted lines on either side of the mean represent the standard deviation.

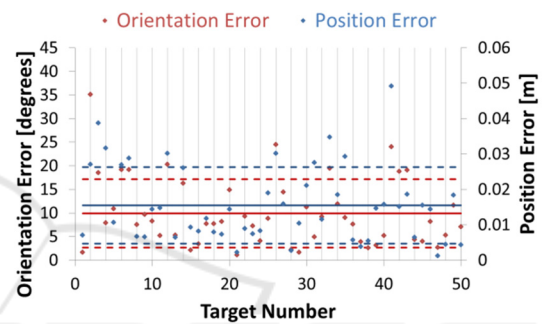


Figure 6: Simulation results for the fifty points experiment for a starting point at one of the boundary extrema.

The next set of simulations were conducted for continuous targets, i.e. the target points are locally adjacent and therefore forms a continuous path. As the target points are close by, the IS solver can output a solution in one iteration. Two such paths were used for evaluation. The first one is a circular path of radius 0.1 meters, centered at (0.25[m], 0[m], 0[m]), with a fixed orientation parallel to the X axis (Fig. 7). The other path is a fixed point with a continuous change in elevation (0→90→0 degrees) and azimuth (0→180 degrees). Fig. 8 shows the target orientation vectors for this simulation and the corresponding solutions from the IS solver. For both tests, the manipulator starts from the home position (Zero force position). The results of both tests are encapsulated in Table 1.

Table 1: Continuous path results.

Test	Position Error (Mean ± Standard Deviation) [m]	Orientation Error (Mean ± Standard Deviation) [degrees]
Circular Path	0.0085 ± 0.0028	7.33 ± 3.98
Angular Path	0.0118 ± 0.0059	3.21 ± 1.71

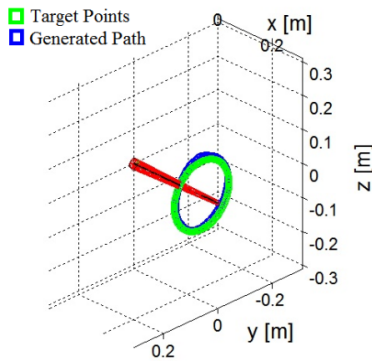


Figure 7: Continuous positional path following with fixed orientation. The target orientation is a vector perpendicular to the YZ plane.

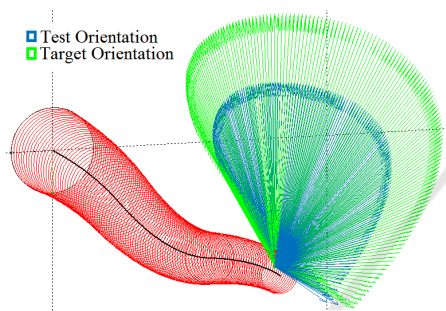


Figure 8: Continuous angular path following.

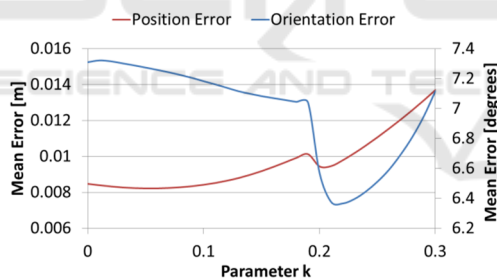


Figure 9: Appended IS solver.

5.2 Appended IS Solver

As mentioned in the subsection 2.1, redundant soft manipulators have certain geometrical properties that could allow smooth motions in the self-motion manifold. The continuous positional path experiment (Fig.7) was again used to test the appended IS solver. Fig. 9 depicts how the modified solver can allow us to trade-off between positional accuracy and orientation accuracy, leading to an improvement in orientation accuracy by 0.95 degrees and reduction of positional accuracy by 1.3 mm.

5.3 Analysis

The proposed methodology for learning the IS of a redundant soft manipulator is an adaptation of the differential IK/IS method. Therefore, we try to make a comparison to the differential IK/IS method. The Jacobian at a point (Equation 2) can be obtained numerically by making infinitesimally small changes in the actuator configuration and observing the corresponding changes in the end effector configuration. Once the Jacobian matrix is obtained, it is inverted to obtain a particular solution to the IK/IS problem. For a redundant manipulator, the Moore-Penrose pseudo inverse will achieve the same. We ignore the null space solutions in this analysis.

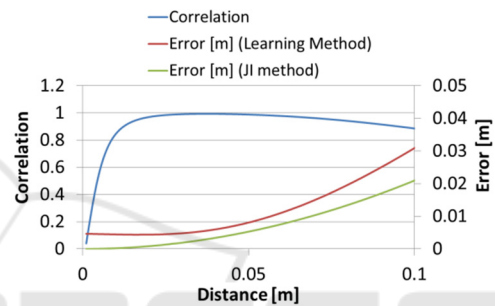


Figure 10: Correlation between the proposed method and JI method for a starting point at the home position.

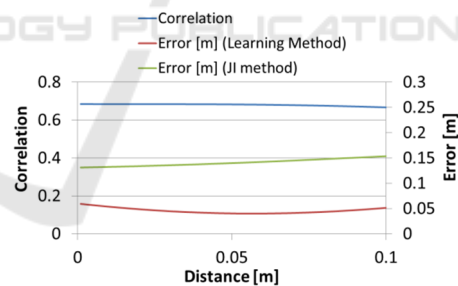


Figure 11: Correlation between the proposed method and Jacobian inverse method starting at a boundary extremum.

We compare the correlation between the solutions provided by a Jacobian pseudo inverse (JI) based method and our proposed method at two points. One is the natural home position and the other is a boundary extremum. The correlation between the Inverse Jacobian method and the proposed method for varying target distance is shown in Fig. 10. We can observe that the correlation between the Jacobian pseudo inverse method and the learned system is high at the home position. This implies that the system tends to learn the ‘shortest path’ solution. It is low at lower

distances possibly because of the added noise. The trend is similar for other points well within the boundary. However for a starting position that lies at one of the extremum of the workspace, the correlation value is less (Fig. 11). The proposed method also performs better than the Inverse Jacobian method.

6 CONCLUSIONS

This paper presents a data driven method for learning the inverse statics mapping of a redundant soft manipulator. The novelty in our methodology arises from our linearized IS problem reformulation and sampling approach while implicitly feeding the learning system with information about the system boundaries. We have demonstrated through simulations that the proposed approach is suitable for static control of high dimensional redundant soft manipulators. We have also tried to address the possibility of utilizing the distinct self-motion manifolds of soft robots and its probable implications. Finally, comparison of the proposed method with commonly used inverse Jacobian method indicates that the learning system generalizes to the ‘shortest path’ solution.

ACKNOWLEDGEMENTS

The authors would like to acknowledge the support by the European Commission through the I-SUPPORT project (HORIZON 2020 PHC-19, #643666). The authors would like to thank Italian Ministry of Foreign Affairs and International Cooperation DGSP-UST for the support through Joint Laboratory on Biorobotics Engineering project.

REFERENCES

- Demers, D., Kreutz-Delgado, K., 1992. Learning Global Direct Inverse Kinematics. *Advances in Neural Information Processing Systems*, 589-595.
- D’Souza, A., Vijayakumar, S., Schaal, S., 2001. Learning Inverse Kinematics. In *Proc IEEE/RSJ International Conference on Intelligent Robots and Systems*, Volume 1, 298 – 303.
- Foresee, F. D., Hagan, M. T., 1997. Gauss-Newton approximation to Bayesian regularization. In *Proc. 1997 International Joint Conference on Neural Networks*, 1930-1935.
- Giorelli, M. et al., 2015. Neural Network and Jacobian Method for Solving the Inverse Statics of a Cable-Driven Soft Arm with Nonconstant Curvature. *IEEE Transactions on Robotics*, 31(4), 823 – 834.
- Jordan, M., Rumelhart, D., 1992. Forward models: supervised learning with distal teacher. *Cognitive Science*, 16(3), 307-354.
- Kapadia, A. D., Walker, I. D., 2013. Self-Motion Analysis of Extensible Continuum Manipulators. *IEEE International Conference on Robotics and Automation*, 1988 – 1994.
- Marchese, A. D. et al., 2014. Design and control of a soft and continuously deformable 2D robotic manipulation system. In *Proc. IEEE International Conference on Robotics and Automation*, 2189-2196.
- Melingui, A. et al., 2014. Neural Networks based approach for inverse kinematic modeling of a Compact Bionic Handling Assistant trunk. *IEEE 23rd Int. Symposium on Industrial Electronic*, 1239-1244.
- Renda, F. et al., 2012. A 3D steady-state model of a tendon-driven continuum soft manipulator inspired by the octopus arm. *Bioinspiration & Biomimetics*, 7(2).
- Renda, F. et al., 2014. Dynamic Model of a Multibending Soft Robot Arm Driven by Cables, *IEEE Transactions on Robotics*, 30(5): 1109 – 1122.
- Rolf, M., Steil J.J., 2013a. Efficient Exploratory Learning of Inverse Kinematics on a Bionic Elephant Trunk, *IEEE Transactions on Neural Networks and Learning Systems*, 25(6), 1147 – 1160.
- Rolf, M., Steil, J.J., 2013b. Explorative learning of right inverse functions: theoretical implications of redundancy. *Neurocomputing*.
- Rus, D., Tolley, M. T., 2015. Design, Fabrication and control of soft robots, *Nature* 521: 467-475.
- Susumu, E.O., Tachi, S., 2001. Inverse kinematics learning by modular architecture neural networks. In *Proc. IEEE International Conference on Robotics and Automation*, 1006-1012.
- Vannucci, L., Cauli, N., Falotico, E., Bernardino, A., Laschi, C., 2014. Adaptive visual pursuit involving eye-head coordination and prediction of the target motion. *14th IEEE-RAS International Conference on Humanoid Robot*, 541-546.
- Vannucci, L., Falotico, E., Di Lecce, N., Dario, P., Laschi, C., 2015. Integrating feedback and predictive control in a Bio-inspired model of visual pursuit implemented on a humanoid robot. *Lecture Notes in Computer Science (including subseries Lecture Notes in Artificial Intelligence and Lecture Notes in Bioinformatics)*, 9222, 256-267.
- Walker, I. D., 2013. Continuous Backbone ‘‘Continuum’’ Robot Manipulators, *ISRN Robotics*, vol. 2013.